Assessing Near-Infrared Quantum Dots for Deep Tissue, Organ, and Animal Imaging Applications

Wen Jiang,[1] *Anupam Singhal,*[1] *Betty Y.S. Kim,*[1] *Jianing Zheng,*[2] *James T. Rutka,*[3] *Chen Wang,*[2] *and Warren C.W. Chan*[1]*
[1]*University of Toronto, Toronto, Ontario, Canada*
[2]*Mount Sinai Hospital, Toronto, Ontario, Canada*
[3]*The Hospital for Sick Children, Toronto, Ontario, Canada*

Keywords:
quantum dots,
in vivo imaging,
near-infrared
imaging,
multiplexed
imaging,
organ,
animal,
targeting,
optical imaging

Semiconductor quantum dots (Qdots) have emerged as novel ultrasensitive optical probes to target, detect, and image fundamental events occurring within the biological system. In particular, near-infrared (near-IR) Qdots holds great promise as in vivo contrast agents for real-time bioimaging capabilities. In this study, biocompatible near-IR Qdots are used to image organs, tissues, and cells. Compared to visible Qdots, we obtained a significant enhancement in signal detection sensitivity for imaging deep tissues and organs. In addition, biomolecules were used to target these optical contrast agents for multiplexed imaging of cells and organs in vivo. The ability to simultaneously distinguish emission profiles of multiple near-IR Qdots will likely emerge as important tools for addressing fundamental questions in molecular biology and in medical sciences. (JALA 2008;13:6–12)

Introduction

Fluorescence-based optical imaging techniques have played a pivotal role in the advancement of biomedical sciences. During the past 20 years, various optical probes have been developed to elucidate complex molecular events inside cells and to detect disease processes.[1–3] Currently used fluorescent probes are dependent on the visible light for detection; however, the use of these traditional markers has been limited for practical bioimaging applications due to several inherent properties of all biological tissues. For example, probe fluorescence can be reduced due to light absorption and scattering events from the intrinsic extinction properties of all constituents of tissues (such as hemoglobin, proteins, and water). Further signal reduction can arise from endogenous fluorophores (such as collagen) that emit within the visible light bandwidth of the electromagnetic spectrum (400–700 nm).[4] To circumvent these limitations, there is great interest in developing novel probes with emission profiles within the near-infrared (near-IR) window. Also referred to as the "diagnostic window" (650–900 nm), the inherent tissue properties at this bandwidth are at their minimum (Fig. 1A).[5]

Various near-IR organic dyes, such as Cyanine and Alexa fluorophore series, have been used to label cells, tissues, and organ systems in vivo.[6,7] However, these organic dyes suffer from low fluorescence quantum yield, broad emission peaks, and rapid photodegradation. Unfortunately, their uses for multiplexed imaging platforms are limited due to their narrow excitation profile. In addition, because only a small number of near-IR organic fluorophores are available, the number of wavelengths that are readily accessible for in vivo multiplexed fluorescence imaging platforms remains a major limitation.

*Correspondence: Warren C.W. Chan, Ph.D., University of Toronto, Institute of Biomaterials & Biomedical Engineering, 164 College St., 408 Toronto, ON M5S 3G9; Phone: +1.416.946.8416; Fax: +1.416.978.4317; E-mail: warren.chan@utoronto.ca

1535-5535/$32.00

doi:10.1016/j.jala.2007.09.002

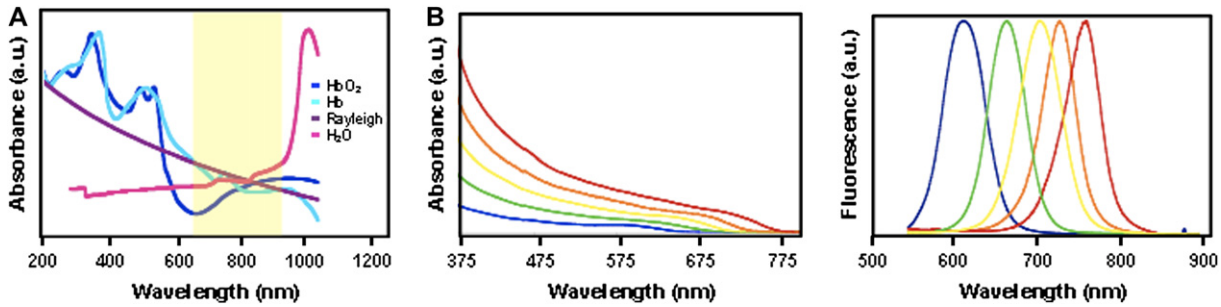

Figure 1. Synthesis and characterization of biocompatible near-infrared (near-IR) for ultrasensitive in vivo imaging applications. (A) Near-IR window for in vivo imaging. The absorption profiles and scattering intensity of major tissues and blood components are at their minimum within the near-IR window. Abbreviations: Hb, hemoglobin; HbO_2, Oxygenated hemoglobin; Rayleigh, Rayleigh Scattering. (B) Absorbance and emission profile of near-IR quantum dots.

During the past decade, semiconductor nanocrystals or quantum dots (Qdots) have generated much interest in the biomedical imaging community.[8,9] By exploiting the tunable optical properties of Qdots, intrinsic limitations of organic fluorophores can be surpassed. Due to enhanced quantum mechanical effects that occur at the nanoscale, the emission profiles of Qdots can be controlled during chemical synthesis by manipulating their size, shape, and material composition. Furthermore, Qdots are approximately 20 times brighter than most organic dyes and are much more resistant to photodegradation. Importantly, the broad absorption profile allows different wavelength-emitting Qdots to be excited using a single laser source for multiplexed capabilities.[10] Therefore, the unique physical properties of Qdots render them as superior multiplexed optical probes for time-lapsed and ultrasensitive biomedical imaging applications.

Currently, visible Qdots have been well characterized and produced as optical probes for bioassay applications.[11] In contrast, near-IR Qdots have not yet been incorporated for biomedical applications due to several fundamental challenges that remain unaddressed. Although various near-IR Qdot synthetic methods have been proposed, their low quantum yield and their rapid photodegradation upon continuous optical excitation remain a major limitation. Yet, another fundamental problem is the inability to interface these inorganic fluorophores with biological molecules, such as DNA and proteins, for targeted detection and imaging capabilities.[12,13] In our previous study, we developed a novel synthetic approach for producing a highly luminescent, monodisperse, and photostable near-IR Qdots composed of $CdTe_xSe_{1-x}$/CdS alloyed structure.[14] In this article, we investigated the potential use of these near-IR Qdots for deep tissue and bioimaging applications. The characterization of improved signal detection sensitivity in tissues and organs will be presented. In addition, for the first time, we demonstrate the ability to use these near-IR Qdots for multiplexed in vivo imaging. Potentially, these near-IR Qdots could hold significant promise for optical-based diagnostic, detection, and imaging applications.

Materials and Methods

Synthesis of Near-IR Qdots

Highly luminescent near-IR Qdots composed of $CdTe_xSe_{1-x}$/CdS core/shell were prepared using a high-temperature organometallic approach.[14] Briefly, 20 g of tri-*n*-octylphosphine oxide (TOPO, tech. 90% purity) was placed in a three-neck reaction flask and filled with argon gas. The flask was heated to 150 °C, which causes the TOPO to melt. At this point, 60 μmol of dimethylcadmium (min. 97% purity) was then injected into the flask and allowed to stir for 15 min. The temperature of the reaction flask was then raised to 325 °C, at which point specific amounts of chalcogenide precursor solutions were injected. Depending on the desired final emission wavelength, different amount of Te and Se precursors were injected. To examine the optical properties of Qdots during synthesis, aliquots were periodically taken from the reaction flask for absorbance and photoluminescence spectra measurements using UV−vispectrophotometer and fluorometer, respectively. Once the Qdots reached a desired size (as indicated by the measured peak emission wavelength), the reaction flask was removed from the heat source to stop the reaction. Passivation of the $CdTe_xSe_{1-x}$ Qdots core with a CdS shell was achieved by drop-wise injection of 400 μL mixture of tri-*n*-octylphosphine sulphide solution at a lower temperature. Once the capping process was finished, the final solution was then cooled to room temperature and washed with methanol.

Water Solubilization

Water solubilization of organometallic-synthesized near-IR Qdots was achieved using bifunctional molecule mercaptoundecanoic acid (MUA, 95%) to replace the hydrophobic surface TOPO ligands.[15] In a typical reaction, Qdots were mixed with excess of MUA at a molar ratio of ~1:20,000 and stirred overnight to displace surface TOPO molecules. The MUA-coated Qdots are soluble in intermediate solvents such as dimethyl sulphoxide. DL-lysine was then used to cross-link MUA surface molecules onto Qdots by using 1,3-dicyclohexylcarbodiimide (99%) mediated chemistry.

This cross-linking step results in the formation of stable capsule like layer that fully protects the inner Qdots from the aqueous environment. Purification of the Qdots from excess reactants was achieved via acetone precipitation and centrifugation. The supernatant that contains excess reactants was discarded, whereas the pellet containing near-IR-emitting Qdots can be dried as powder or dissolved in aqueous buffer such as Z-(N-morpholino) ethanesulfonic acid (MES) or phosphate buffered saline (PBS) for future use.

Bioconjugation and Cell Culture

Conjugation of near-IR Qdots with proteins requires the formation of stable covalent linkage. For this purpose, we selected carbodiimide-mediated cross-linking chemistry.[16] For typical transferrin conjugation, Qdots were first dissolved in MES buffer (pH 6) at 10 mg/mL. Correct amounts of ethyl-3-(3-dimethylaminopropyl) carbodiimide hydrochloride (EDC) and *N*-hydroxysulfosuccinimide (sulfo-NHS) were added to the Qdots solution to obtain a final concentration of 2 and 5 mM, respectively. The solution was allowed to react while mixing for 15 min, upon which transferrin dissolved in 0.1 M sodium phosphate buffer (pH 7.5) was then added to initiate the cross-linking process between the Qdots and proteins. The final reaction solution was stirred for 1 h. The Qdots–protein bioconjugates was extracted after the removal of excess reactants and byproducts through gel filtration column purification.

For intracellular staining, HeLa cells (30–50% confluency plated on 15 × 100 mm tissue culture dishes) were incubated overnight with Qdots bioconjugates at 37 °C. These cells were plated using Dulbecco's Minimum Essential medium with 10% Fetal Bovine Serum, 1% penicillin, and 1% amphotericin B. After Qdot incubation, HeLa cells were trypsinized and washed with PBS to remove any unbound Qdots. The Qdot-stained cells were then fixed using 4% paraformaldehyde, followed by DAPI stain of the nucleus. Bright-field and epifluorescence images of cells were then captured using an Olympus IX71 microscope.

Characterization

Animals were used in accordance with an approved institutional protocol. Briefly, 4- to 6-week-old ICR mouse were sacrificed to dissect various tissues and organs including the femur and the heart. The isolated organs were placed in PBS and near-IR Qdots (~100 μL of diluted solution) were injected directly into organ cavities. For tissue-penetration studies, Qdot-injected organs were imaged using a Zeiss LSM 510 confocal microscope with a Photo Multiplier Tube detector. The collected optical signals were analyzed using ImagePro-Plus 5.0 software. For in vivo multiplexed imaging experiments, near-IR Qdots were injected subcutaneously into the chest and abdominal cavities of anesthetized newborn ICR mice. Fluorescence images were then obtained using a Leica MZ FLIII stereomicroscope mounted with Charge-Coupled Device camera.

Results

Optical and Physical Characterization

Highly luminescent, monodisperse, and photostable near-IR Qdots were prepared using an organometallic approach. By varying the ratio of Te to Se composition, we were able to tune the emission wavelength of these Qdots from 650 to 850 nm (Fig. 1B). To improve the stability of these Qdots, an additional CdS coating layer was grown on the nanocrystal surface. This passivating layer protects the $CdTe_xSe_{1-x}$ core from rapid degradation from processes such as photooxidation. Upon continuous optical excitation, photostability of the capped $CdTe_xSe_{1-x}$/CdS Qdots was significantly enhanced as compared to the uncapped $CdTe_xSe_{1-x}$ Qdots.[13]

By replacing the organic ligands on the Qdots surface with bifunctional molecules, Qdots were made water soluble. Carboxylate groups on the surface of these Qdots are used to conjugate bio-recognition molecules such as oligonucleotides and proteins for targeting purposes. Figure 2A schematically illustrates the entire procedure for preparing biocompatible near-IR Qdot. Transmission electron microscopy (TEM) and fluorescence microscopy confirmed that these Qdots maintained their monodispersity during the surface modification process with no significant loss in the fluorescence emission (Fig. 2B–D). The typical quantum yield for bioconjugated Qdots was measured to be approximately 30%. This value is approximately two- to threefolds higher than any comparable biocompatible near-IR Qdots prepared using previously described methods.[17] Importantly, these bioconjugated Qdots were bright enough to be imaged using an epifluorescence microscope at a single dot level (Fig. 2D, E).

Cell Fluorescence Staining

For multiplexed, long-term and target-specific labeling of cellular components, we conjugated transferrin, an iron transport protein, to the Qdot surface using EDC-mediated catalysis. Incubation of bioconjugated near-IR Qdots with HeLa cells for 3 h resulted in a significant uptake of Qdots into cytoplasmic vesicles (Fig. 3A–C). No detectable signals were observed with unconjugated Qdots or with Qdots bioconjugated to an irrelevant protein (bovine serum albumin). Therefore, the observed enhanced fluorescence within cells was due to the trapping of Qdots in the endocytic intracellular vesicles.[18] In addition, these Qdots were observed to maintain their fluorescence intensity after overnight incubation with cells, demonstrating their stability against environment-induced degradation.

For targeted multiplexed imaging applications, cell-labeling experiments were performed as described in the previous section. Using near-IR Qdots of two unique emission wavelengths (660 and 750 nm), we conjugated these Qdots to transferrin. By using an appropriate filter system with no spectral overlap, we were able to label two distinct populations of HeLa cells (Fig. 3D–I). Due to the narrow emission profile of our near-IR Qdots, we were able to spectrally identify and label specific targets of interests. Using our near-IR

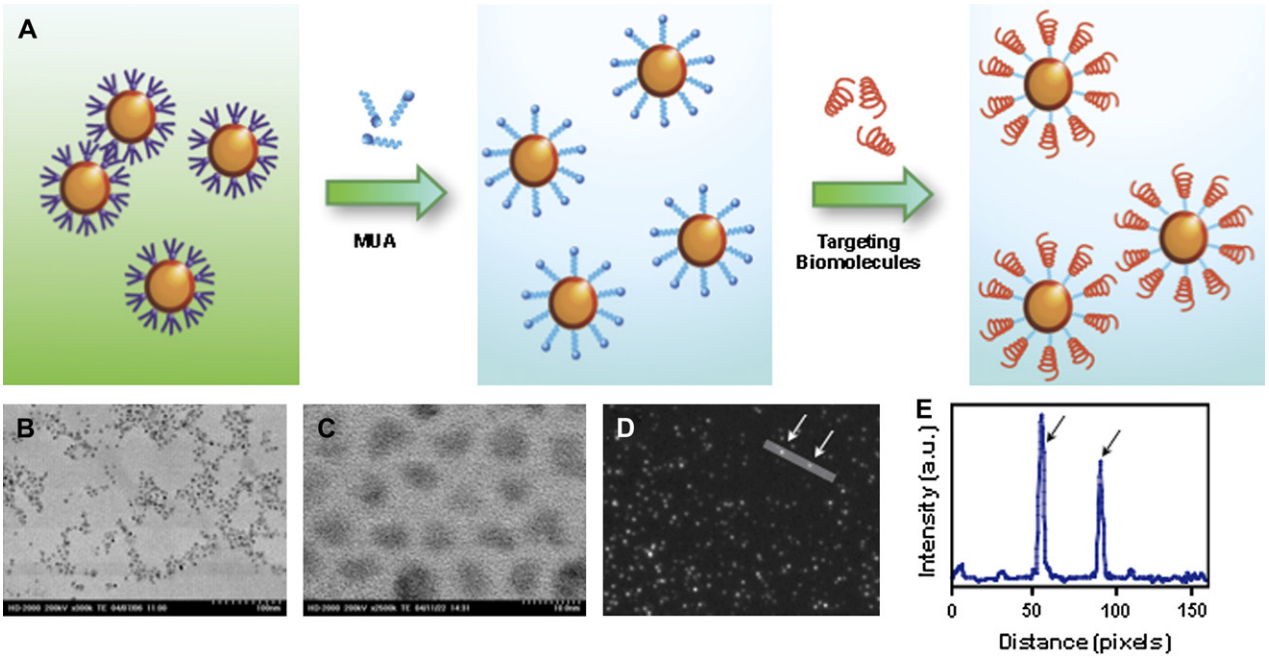

Figure 2. Surface modification and characterization of near-infrared (near-IR) quantum dots (Qdots). (A) An illustration demonstrating the synthetic process for preparing biocompatible near-IR Qdots. The tri-*n*-octylphosphine oxide-coated organic Qdots were first made water soluble by exchanging with the bifunctional molecule mercaptoundecanoic acid (MUA). Water-soluble Qdots can then be conjugated with biomolecules such as proteins and DNA for targeted imaging applications. (B) Transmission electron microscopy (TEM) images of monodisperse organic-soluble Qdots. (C) TEM images of monodisperse water-soluble Qdots. (D, E) Highly luminescent near-IR Qdots can be imaged at the single Qdot level. (D) The white arrows indicate fluorescence signals corresponding to single Qdots. (E) The black arrows indicate corresponding intensity peaks of the two single near-IR Qdots.

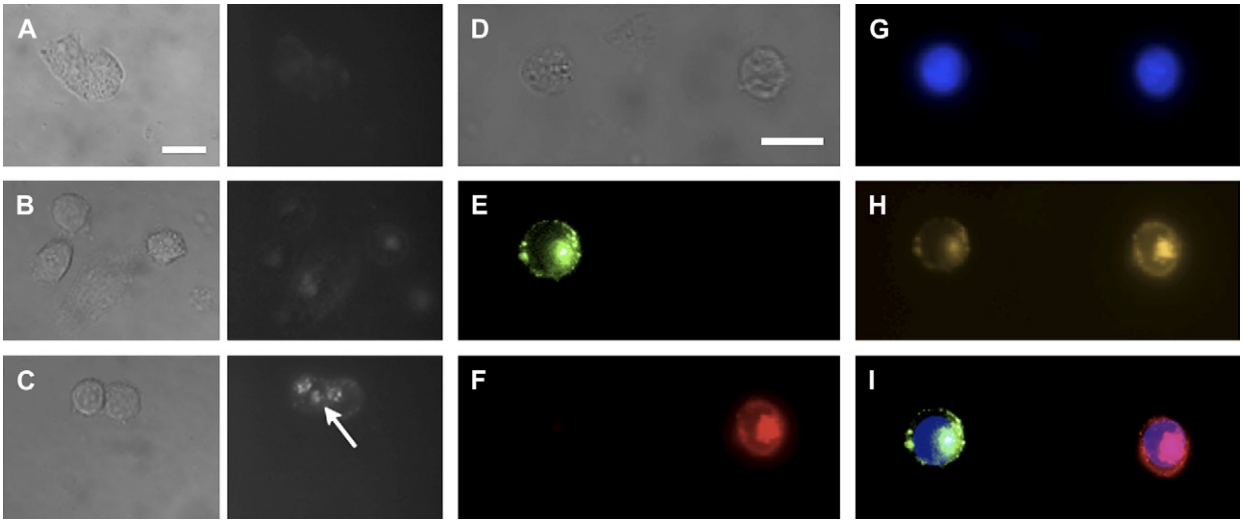

Figure 3. Fluorescent labeling of intracellular components using near-infrared (near-IR) quantum dots (Qdots). (A–C) HeLa cells were incubated with (A) free Qdots, (B) bovine serum albumin (BSA) conjugated Qdots, and (C) transferrin-conjugated Qdots. Qdots used for these experiments emit at 750-nm wavelength. No significant fluorescence signals were detected in cells incubated with free Qdots and BSA-conjugated Qdots. In contrast, near-IR Qdots can be observed within vesicle-like structures (arrow). Corresponding bright-field images are shown on the left panel for each fluorescence images. (D–I) In vitro multiplexed imaging using near-IR Qdots. Two different sets of HeLa cells were labeled with transferrin conjugated to Qdots emitting at 650- or 750-nm wavelengths. (D) Bright-field image of two cells and (E–I) the corresponding fluorescence images of the same two cells were obtained. The different cell populations can then be identified using (E) 650-nm bandpass filters (F) 750-nm bandpass filters. (G) Nuclear staining with DAPI. (H) By using 600-nm longpass filter set, we observed Qdot localization within the perinuclear region of cells. (I) Superimposed image of E, F, and G. (Scale bar = 10 μm).

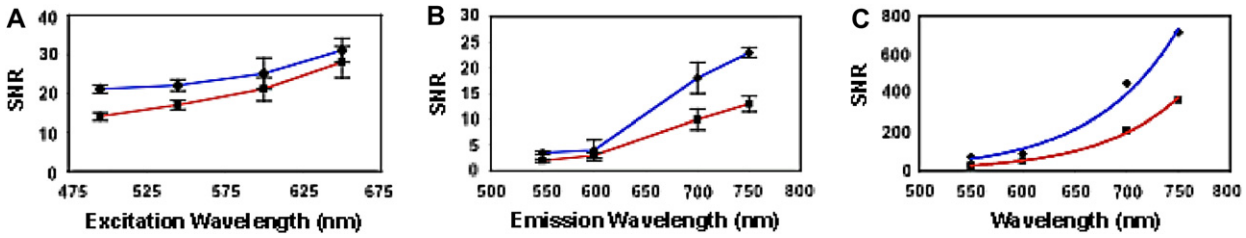

Figure 4. Tissue and animal imaging using near-infrared (near-IR) quantum dots (Qdots). (A–C) Signal-to-noise ratio (SNR) analysis of mouse femur and heart (red and blue, respectively) imaging with near-IR Qdots. SNR for imaging organs using (A) varying excitation wavelengths and (B) Qdot emission wavelengths. (C) Overall improvement in SNR attributed to both longer excitation and emission wavelengths. This resulted in almost 10-fold enhancement in the signal sensitivity for 750-nm emitting Qdots compared to 550-nm emitting Qdots.

Qdots, it is possible to resolve at least five to six near-IR Qdots with a proper filter system. The same is not possible with currently available organic fluorophores due to their broad emission profile. In addition, with the development of contrast agents in the second near-IR/IR window (1025–1150, 1225–1370, and 1610–1710 nm),[19] it may be possible to simultaneously detect, image, and monitor more than 10 unique targets of interests with minimal signal interference.

Tissue Imaging and Penetration Depth Study

To quantitatively study the optimal-achievable signal sensitivity and tissue depth penetration of our near-IR Qdots, we used standard fluorescence imaging techniques to visualize and compare visible Qdots with near-IR Qdots. Before injection of these Qdots into isolated heart and femur, each Qdots solution was calibrated to obtain a comparable fluorescence intensities for a given excitation wavelength. The overall signal-to-noise ratio (SNR) was then determined by measuring the signal intensities for organs treated with and without Qdots. The highest optical sensitivity for Qdots within organs was observed when Qdot excitation and emission occurred in longer wavelength (Fig. 4A, B). As compared to visible Qdots, the overall improvement in SNR using near-IR emitting Qdots was estimated to be at least 10 times higher for organs and for in vivo whole animal imaging (Fig. 4C). To study the maximum imaging penetration

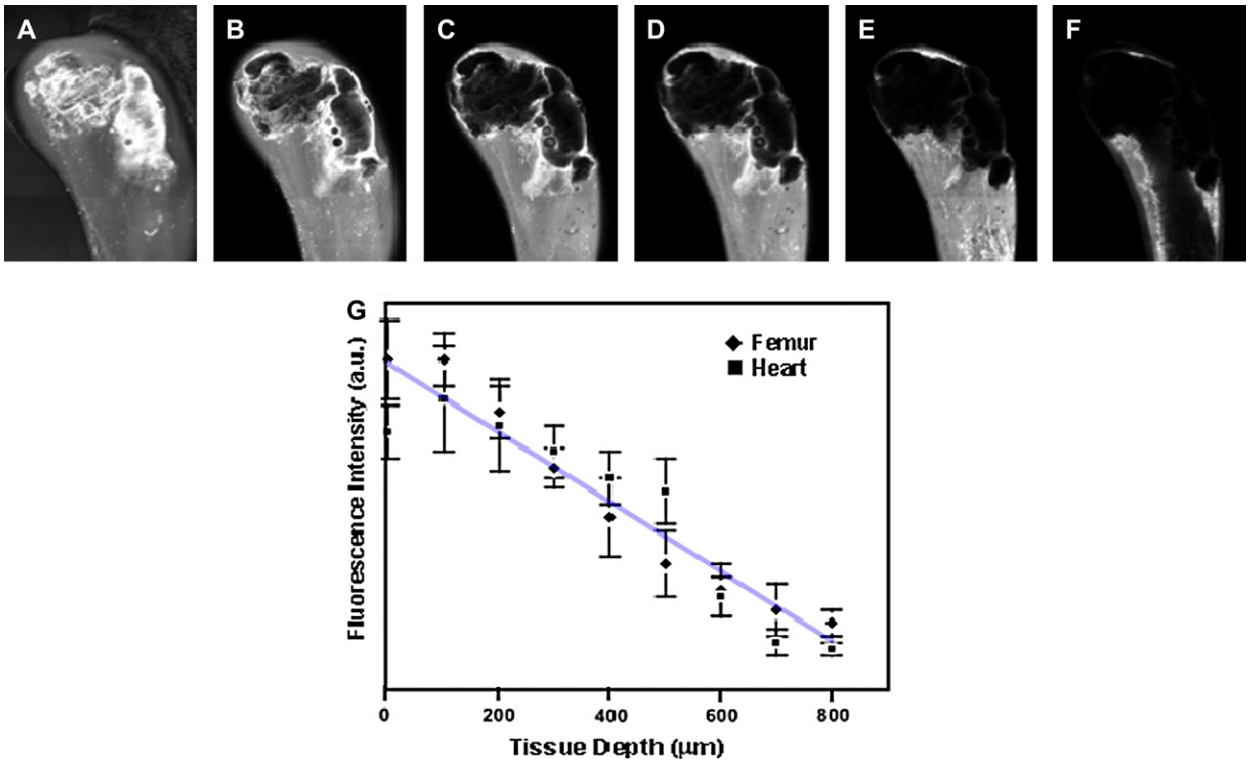

Figure 5. Deep tissue laser confocal fluorescence imaging using near-infrared (near-IR) quantum dots (Qdots). (A–F) Laser confocal images of mouse femur injected with near-IR Qdots. Each image represents a different tissue depth. (G) Tissue-penetration depth analysis of near-IR Qdots in both heart and femur using confocal microscopy. Optical signals are detectable up to 0.8 mm of tissue depth without any adjustments made on the laser power or optical gain.

depth achievable, we injected 750-nm emitting near-IR Qdots into isolated hearts and femurs of mice. These organs were analyzed using a serial-depth confocal microscopy imaging system (Fig. 5A–F). Fluorescence signals were readily detectable up to 0.8 mm in both organs without the need to increase excitation power or optical gain (Fig. 5G). The observed depth of probe detection exceeds currently used imaging depth of 500 and 800 μm for confocal and two-photon microscopy, respectively. Such imaging depth can be further improved by using specific filter set and camera and detectors with higher quantum efficiency in the near-IR range. These results demonstrate that near-IR Qdots may potentially be used as optical agents for high-resolution confocal and two-photon microscopy to image deep tissue specimens without significantly losing optical signal intensity.

Multiplexed Imaging

To further demonstrate the ability to conduct multiplexed imaging in live animals, two different wavelength-emitting Qdots (660 and 750 nm) were injected into the left and right chest cavity of a mouse. Fluorescence signals from the two injected areas were very bright compared to the background. Also, different Qdot signals were easily differentiated using bandpass filters (Fig. 6). Although still preliminary, various studies have shown the lack of acute cytotoxicity of Qdots with the proper surface coating layer.[19] Despite the uncertainty of effects due to chronic exposure, single-dose rapid detection, imaging, and diagnosis using near-IR remain a viable option. These near-IR Qdots can also be potentially used for real-time image-guided intraoperative guidance platforms. For example, targeted near-IR Qdots can serve as highly sensitive and specific in vivo contrast agents to detect tumor cells for optimal resection or for diagnostic biopsies.

Conclusion

Near-IR Qdots holds great potential as contrast agents for in vivo imaging of deep tissues or as noninvasive molecular imaging platforms. In this article, we demonstrate the use of newly developed near-IR Qdots for biolabeling, deep tissue, and multiplexed in vivo imaging applications. These Qdots were successfully conjugated to biological molecules for targeted cell-labeling applications. Potentially, these Qdots can be implemented for multiplexed and time-lapsed in vivo molecular imaging platforms. By comparing these near-IR Qdots to their visible counterparts using fluorescence and laser confocal microscopy, the detection sensitivity was enhanced by at least 10 folds.[14,20] Further improvements can be made by developing more sensitive detection systems in the near-IR region. Finally, we also demonstrated the ability to perform multiplexed in vivo imaging using these near-IR Qdots. Multiplexing can potentially allow researchers to perform real-time tracking of multiple biological molecules in live animals with minimal loss in optical detection sensitivity. The ability to spectrally distinguish unique sets of near-IR Qdots can lead to improvements in earlier detection of diseases such as cancer, where multiple markers can be detected

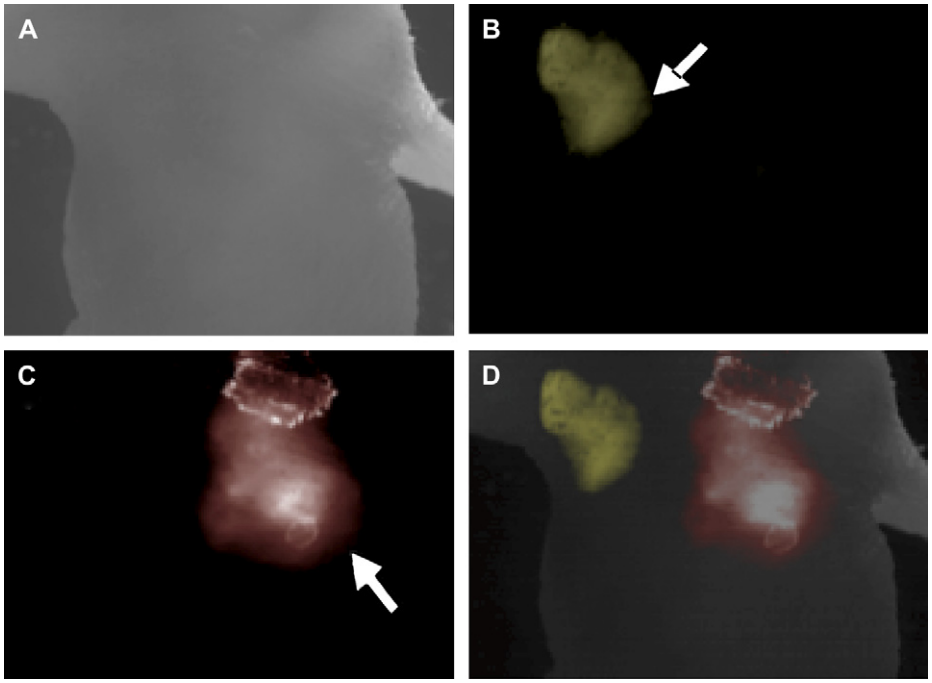

Figure 6. Multiplexed in vivo imaging using near-infrared (near-IR) quantum dots (Qdots). (A) Bright-field images. (B) Fluorescence images obtained from mouse injected with 650-nm emitting Qdots (arrow) using 650/50 bandpass filters. (C) Fluorescence images from the same mouse injected with 750-nm emitting Qdots (arrow) using 750/50 bandpass filters. (D) Superimposed images of (A, B, and C) demonstrate multiplexed near-IR Qdots at the injection site relative to normal mouse anatomy.

simultaneously using a bioconjugated near-IR Qdots cocktail.

Acknowledgments

We wish to thank Dr. Paul Kongkham for helpful discussions, Dr. Neil Coombs with TEM, and James Yonkman with confocal microscopy. This work is supported by the Canadian Institute of Health Research (C.W., J.T.R., W.C.W.C.), Natural Sciences and Engineering Council of Canada (W.J., B.Y.S.K., W.C.W.C.), Canada Foundation for Innovation (W.C.W.C.), Ontario Innovation Trust (C.W., W.C.W.C.), the University of Toronto (J.T.R., W.C.W.C.) Surgeon Scientist Program, The University of Toronto (B.Y.S.K.), and Ministry of Health Funding (B.Y.S.K.).

References

1. Rieder, C. L.; Khodjakov, A. Mitosis through the microscope: Advances in seeing inside live dividing cells. *Science* **2003,** *300*, 91−96.
2. Truong, L.; et al. Quantitative fluorescence in situ hybridization in lung cancer as a diagnostic marker. *J. Mol. Diagn.* **1999,** *1*, 33−37.
3. Voura, E. B.; Jaiswal, J. K.; Mattoussi, H.; Simon, S. M. Tracking metastatic tumor cell extravasation with quantum dot nanocrystals and fluorescence emission-scanning microscopy. *Nat. Med.* **2004,** *10*, 993−998.
4. Weissleder, R. A clearer vision for in vivo imaging. *Nat. Biotechnol.* **2001,** *19*, 316−317.
5. Frangioni, J. V. In vivo near-infrared fluorescence imaging. *Curr. Opin. Chem. Bio.* **2003,** *7*, 626−634.
6. Mujumdar, R. B.; Ernst, L. A.; Mujumdar, S. R.; Lewis, C. J.; Waggoner, A. S. Cyanine dye labeling reagents: Sulfoindocyanine succinimidyl esters. *Bioconjugate Chem.* **1993,** *4*, 105−111.
7. Hilger, I.; et al. Near-infrared fluorescence imaging of HER-2 protein over-expression in tumour cells. *Eur. Radiol* **2004,** *14*, 1124−1129.
8. Chan, W. C.; Nie, S. Quantum dot bioconjugates for ultrasensitive nonisotopic detection. *Science* **1998,** *281*, 2016−2018.
9. Bruchez, M. Jr.; Moronne, M.; Gin, P.; Weiss, S.; Alivisatos, A. P. Semiconductor nanocrystals as fluorescent biological labels. *Science* **1998,** *281*, 2013−2016.
10. Klostranec, J. M.; Chan, W. C. Quantum dots in biological and biomedical research: Recent progress and present challenges. *Adv. Mat.* **2006,** *18*, 1953−1964.
11. Bailey, R. E.; Nie, S. Alloyed semiconductor quantum dots: Tuning the optical properties without changing the particle size. *J. Am. Chem. Soc.* **2003,** *125*, 7100−7106.
12. Kim, S.; Fisher, B.; Eisler, H. J.; Bawendi, M. G. Type-II quantum dots: CdTe/CdSe(core/shell) and CdSe/ZnTe(core/shell) heterostructures. *J. Am. Chem. Soc.* **2003,** *125*, 11466−11467.
13. Jiang, W.; Singhal, A.; Zheng, J.; Wang, C.; Chan, W. C. W. Optimizing the synthesis of red- to near-IR-emitting CdS-capped CdTexSe1-x alloyed quantum dots for biomedical imaging. *Chem. Mater.* **2006,** *18*, 4845−4854.
14. Jiang, W.; Mardyani, S.; Fischer, H.; Chan, W. C. W. Design and characterization of lysine cross-linked mercapto-acid biocompatible quantum dots. *Chem. Mater.* **2006,** *18*, 872−878.
15. Hermanson, G. T. *Bioconjugate Techniques* Ch. 3 Academic Press: New York; 1996.
16. Kim, S.; Lim, Y. T.; Soltesz, E. G.; De Grand, A. M.; Lee, J.; Nakayama, A.; Parker, J.; Mihaljevic, T.; Laurence, R. G.; Dor, D. M.; Cohn, L. H.; Bawendi, M. G.; Frangioni, J. V. Near-infrared fluorescent type II quantum dots for sentinel lymph node mapping. *Nat. Biotechnol.* **2004,** *22*, 93−98.
17. Jaiswal, J. K.; Mattoussi, H.; Mauro, J. M.; Simon, S. M. Long-term multiple color imaging of live cells using quantum dot bioconjugates. *Nat. Biotechnol.* **2003,** *21*, 47−51.
18. Lim, Y. T.; Kim, S.; Nakayama, A.; Stott, N. E.; Bawendi, M. G.; Frangioni, J. V. Selection of quantum dot wavelengths for biomedical assays and imaging. *Molecular Imaging* **2003,** *2*, 50−64.
19. Fischer, H. C.; Liu, L.; Pang, K. S.; Chan, W. C. W. Pharmacokinetics of nanoscale quantum dots: In vivo distribution, sequestration, and clearance in the rat. *Adv. Funct. Mater.* **2006,** *16*, 1299−1305.
20. Gao, X.; Cui, Y.; Levenson, R. M.; Chung, L. W. K.; Nie, S. In vivo cancer targeting and imaging with semiconductor quantum dots. *Nat. Biotechnol.* **2004,** *22*, 969−976.